Open Journal of Microphysics, 2012, 2, 19-26
http://dx.doi.org/10.4236/ojm.2012.22003 Published Online May 2012 (http://www.SciRP.org/journal/ojm)

Production of *J*/Ψ-Particles at RHIC and LHC Energies: An Alternative "Psi"-Chology

P. Guptaroy[1*], Goutam Sau[2], S. K. Biswas[3], S. Bhattacharyya[4]
[1]Department of Physics, Raghunathpur College, Raghunathpur, India
[2]Beramara Ram Chandrapur High School, Alipore, India
[3]West Kodalia Adarsha Siksha Sadan, Kolkata, India
[4]Physics and Applied Mathematics Unit (PAMU), Indian Statistical Institute, Kolkata, India
Email: *gpradeepta@rediffmail.com, {sau_goutam, sunil_biswas2004}@yahoo.com, bsubrata@isical.ac.in

Received February 15, 2012; revised March 22, 2012; accepted April 5, 2012

ABSTRACT

We attempt here to understand successfully some crucial aspects of *J*/Ψ-production in some high energy nuclear collisions in the light of a non-standard framework outlined in the text. It is found that the results arrived at with this main working approach here is fairly in good agreement with both the measured data and the results obtained on the basis of some other models of the 'standard' variety. Impact and implications of this comparative study have also been precisely highlighted in the end.

Keywords: Relativistic Heavy Ion Collisions; Inclusive Production; Charmed Meson

1. Introduction

The study of the *J*/Ψ-mesons in ultra-relativistic heavy ion collisions has consistently been considered to be a potentially powerful tool for studying the properties of the hypothetical 'hot and dense matter' created in these collisions. Predictions about the *suppression* of *J*/Ψ-meson production in the nuclear collision, at certain stages [1] and an anomalous *enhancement* at certain other stage as well [2] are always treated as very powerful diagnostics. The deciding factor, in terms of the Standard Model (SM), in both the cases, is the number of charm-anticharm ($c\bar{c}$) pairs ($N_{c\bar{c}}$) created in the early stage of hard parton collisions in $A + A$ (or in $A + B$) reactions. On the basis of it, one might arrive at the assumptions of the *J*/Ψ-*suppression* (at $N_{c\bar{c}} < 1$) and the *J*/Ψ-*enhancement* (at $N_{c\bar{c}} > 1$) effects.

In the past, [3-5] we had constantly refrained from giving such undue importance to any controversy about either suppression/enhanced suppression or an enhancement of *J*/Ψ mesons in reality. Rather our primary intent would centre around understanding and interpreting the nature of data of inclusive cross-sections and some other important observables of *J*/Ψ mesons in BNL-RHIC and CERN-LHC experiments. In fact, we have an altogether different and heretic view (which will be outlined very briefly in the next section) about the mechanism of *J*/Ψ production in high energy particle and nuclear collisions.

We define our objectives here as: 1) to explain the main and major features of the latest data on *J*/Ψ-production in BNL-RHIC and CERN-LHC experiments from the proposed alternative approach built up by us in a set of previous works done in the both the remote and recent past [6,7] and 2) to compare our model-based calculations with some other competing models.

Our plan of work presented here is as follows. In Section 2, we provide brief outlines of the models chosen for this study. The Section 3 provides very brief outlines of the models which are founded on the gantlets of assumptions of the "Standard"-model and which have been reckoned with for the sake of comparison. In Section 4 we give the results and general discussion. And in the last section (Section 5) we offer the final remarks and the conclusions arrived at.

2. The Main Approach: An Outline

In the present work, we will make use of a theoretical model to interpret some of the latest and topical observables of the *J*/Ψ production which were measured and reported by the different groups in the Relativistic Heavy Ion Collider (RHIC) and Large Hadron Collider (LHC) experiments in the recent past. The model has a modest degree of dynamical basis and some prior check-ups with data [3-5]. It is called here as the sequential chain model (SCM).

The outline and features of the model we use here are obtained, in the main, from our previous works [3-5].

*Corresponding author.

According to this model, high energy hadronic interactions boil down, essentially, to the pion-pion interactions; as the protons are conceived in this model as $p = (\pi^{+}\pi^{0}\vartheta)$, where ϑ is a spectator particle needed for the dynamical generation of quantum numbers of the nucleons. The multiple production of *J*/Ψ-mesons in a high energy proton-proton collisions is described in the following way. The secondary π-meson or the exchanged ϱ-meson emit a free ω-meson and pi-meson; the pions so produced at high energies could liberate another pair of free ϱ and trapped ω-mesons (in the multiple production chain). These so-called free ϱ and ω-mesons decay quite a fast into photons and these photons decay into Ψ or Ψ′ particles, which, according to this alternative approach is a bound state of $\Omega\bar{\Omega}$ or $\Omega'\bar{\Omega}'$ particles.

The inclusive cross-section of the Ψ-meson produced in the *pp* collisions given by

$$E\frac{d^3\sigma}{\mathrm{d}p^3}\Big|_{p+p\to J/\psi+X} \cong C_{J/\psi}\frac{1}{p_T^{N_R}}\exp\left(\frac{-5.35\left(p_T^2+m_{J/\psi}^2\right)}{\left\langle n_{J/\psi}\right\rangle_{pp}^2\left(1-x\right)}\right)\exp\left(-1.923\left\langle n_{J/\psi}\right\rangle_{pp}x\right), \quad (1)$$

where the expression for average multiplicity for Ψ-particles in *pp* scattering would be given by

$$\left\langle n_{J/\psi}\right\rangle_{pp} = 4\times10^{-6}s^{1/4} \quad (2)$$

In the above expression, the term $\left|C_{J/\psi/}\right|$ is a normalisation parameter and is assumed here to have a value ≈ 0.09 for Intersecting Storage Ring (ISR) energy, and it is different for different energy and for various collisions. The terms p_T, x and $m_{J/\psi}$ represent the transverse momentum, Feynman scaling variable and the rest mass of the *J*/Ψ particle respectively. Moreover, by definition, $x = 2\,p_L/\sqrt{s}$ where p_L is the longitudinal momentum of the particle. The *s* in Equation (2) is the square of the cm energy.

The second term in the right hand side of the Equation (1), the constituent rearrangement term arises out of the partonic rearrangements inside the proton. It is established that hadrons (baryons and mesons) are composed of few partons. These rearrangements mean undesirable loss of energy, in so far as the production mechanism is concerned. The choice of N_R would depend on the following factors: 1) the specificities of the interacting projectile and target; 2) the particularities of the seconddaries emitted from a specific hadronic or nuclear interaction and 3) the magnitudes of the momentum transfers and of a phase factor (with a maximum value of unity) in the rearrangement process in any collision. The parametrisation is to be done for two physical points, viz., the amount of momentum transfer and the contributions from a phase factor arising out of the rearrangement of the constituent partons. Collecting and combining all these, we propose the relation to be given by [8]

$$N_R = 4\left\langle N_{\mathrm{part}}\right\rangle^{1/3}\theta, \quad (3)$$

where $\left\langle N_{\mathrm{part}}\right\rangle$ denotes the average number of participating nucleons and θ values are to be obtained phenomenologically from the fits to the data-points [9].

In order to study a nuclear interaction of the type $A + B \to Q + x$, where *A* and *B* are projectile and target nucleus respectively, and *Q* is the detected particle which, in the present case, would be *J*/Ψ-mesons, the SCM has been adapted, on the basis of the suggested Wong [10] work to the Glauber techniques. The inclusive cross-sections for *J*/Ψ production in different nuclear interactions of the types $A + B \to J/\Psi + X$ in the light of this modified Sequential Chain Model (SCM) can then be written in the following generalised form as:

$$E\frac{d^3\sigma}{\mathrm{d}p^3}\Big|_{A+B\to J/\psi+X} \cong a_{J/\psi}\frac{1}{p_T^{N_R}}\exp\left(-c\left(p_T^2+m_{J/\psi}^2\right)\right)\exp\left(-1.923\left\langle n_{J/\psi}\right\rangle_{pp}x\right), \quad (4)$$

where $a_{J/\psi}$, N_R and c are the factors to be calculated under certain physical constraints. The set of relations to be used for evaluating the parameters $a_{J/\psi}$ is given below.

$$a_{J/\psi} = C_{J/\psi}\frac{3}{2\pi}\frac{\left(A\sigma_B + B\sigma_A\right)}{\sigma_{AB}}\frac{1}{1+a'\left(A^{1/3}+B^{1/3}\right)} \quad (5)$$

Here, in the above set of equations, the third factor gives a measure of the number of wounded nucleons *i.e.* of the probable number of participants, wherein $A\sigma_B$ gives the probability cross-section of collision with '*B*' nucleus (target), had all the nucleons of *A* suffered collisions with *B*-target. And $B\sigma_A$ has just the same physical meaning, with *A* and *B* replaced.

Besides, in expression (5), the fourth term is a physical factor related with energy degradation of the secondaries due to multiple collision effects. The parameter a' occurring in Equation (5) above is a measure of the fraction of the nucleons that suffer energy loss. The maximum value of a' is unity, while all the nucleons suffer energy loss. This a' parameter is usually to be chosen [10], depending on the centrality of the collisions and the nature of the secondaries. The "*a*" factor in the expression (5) accommodates a wide range of variation because of the existence of the large differences in the in the normalizations of the *J*/Ψ cross-sections for different types of interactions.

3. Some Competing Models: The Brief Outlines

3.1. The Gluon Saturation Approach

In this approach [11], it is assumed that the nuclear wave functions in very high-energy nuclear collisions can be described by the Color Glass Condensate (CGC). The primary effect is the suppression of *J*/Ψ production and narrowing of the rapidity distribution due to saturation of the gluon fields in heavy ion collisions relative to $p + p$ collisions. In addition, the production mechanism is modified from $p + p$ such that the multigluon exchange diagrams are enhanced in heavy ion reactions. It should be noted that this model does not include any hot medium effects, but does have a free parameter for the overall normalization factor.

3.2. The Quark Coalescence Model (QCM)

The Quark Coalescence Model (QCM) [12], is a two-stage simulation. In stage I the incoming target and projectile nucleon interactions are tracked, a fluid of pre-hadrons is formed and in stage II the produced pre-hadrons interact and decay in a standard relativistic cascade model. The time history of all the collisions recorded in stage I sets up the geometry and initial conditions for stage II. Basic inputs for the simulation are measured hadron-hadron cross-sections, rapidity, transverse momentum and particle multiplicity distributions, of which the last are conforming to KNO scaling. The basic assumption of the model is coalescence of charm quarks and antiquarks into charmonia ($c\bar{c} \rightarrow$ charmonium), which can also be viewed as heavy pre-hadrons in stage I. Only a small percentage of charm quarks are expected to coalesce into bound charmonia *i.e. J*/Ψ, the remainder of such quarks appear ultimately as open charm mesons. At RHIC energies comover suppression of directly produced charmonia is expected to be large, due to the increased particle numbers and densities.

3.3. Double Color Filter-Oriented Approach

A mechanism called double color filtering for $c\bar{c}$ dipoles [13], makes nuclei significantly more transparent in *AA* than *pA* collisions. The assumption of this model is as follows: In the cm of nuclear collision the nuclear disks passing through each other leave behind a cloud of radiated gluons creating a dense matter, which the *J*/Ψ propagates through. In this reference frame the *J*/Ψ full momentum is p_T, which ranges from zero to several GeV in RHIC data. Such a low energy $c\bar{c}$ dipole develops the *J*/Ψ wave function pretty fast, during time t_f < 0.5 fm, which is about the time scale of the medium creation. Thus, what is propagating through the medium is not a small $c\bar{c}$ dipole, but a fully formed *J*/Ψ. The observed nuclear effects in *J*/Ψ production in *AA* collisions is interpreted as a combination of final state interaction (FSI) of *J*/Ψ in the dense medium, and the initial state interaction (ISI) effects in production of *J*/Ψ caused by multiple interactions of the colliding nuclei.

4. The Results

Now let us proceed to apply the chosen model to interpret some recent experimental results of *J*/Ψ-production reported by various groups for different collisions like $p + p$, $d + Au$, $Cu + Cu$, $Au + Au$ at RHIC and $p + p$, $Pb + Pb$ at LHC. Here, the main observables are the invariant yields, rapidity distributions and the nuclear modification factors which would come under purview of the present work.

4.1. *J*/Ψ (Total) Cross-Sections and Rapidity Distribution in $p + p$ Interactions

As the psi-productions are generically treated rightly as the resonance particles, the standard practice is to express the measured *J*/Ψ (total) cross-sections times branching ratio to muon or electrons, *i.e.* for lepton pairs, that is by $B_{u'}\sigma_{p+p}^{J/\psi}$.

By using Expression (4) we arrive at the expressions for the differential cross-sections for the production of *J*/Ψ-mesons in the mid and forward-rapidities (*i.e.* $|y| < 0.35$ and $1.2 < |y| < 2.2$ respectively) in $p + p$ collisions at $\sqrt{s_{NN}}$ = 200 GeV at RHIC.

$$\frac{1}{2\pi p_T} B_{ll'} \frac{d^2\sigma}{\mathrm{d}p_T \mathrm{d}y}\Big|_{p+p\to J/\Psi+X} = 6.1 p_T^{-1.183} \exp\left[-0.13\left(p_T^2 + 9.61\right)\right] \quad \text{for } |y| < 0.35 \tag{6}$$

and

$$\frac{1}{2\pi p_T} B_{ll'} \frac{d^2\sigma}{\mathrm{d}p_T \mathrm{d}y}\Big|_{p+p\to J/\Psi+X} = 6.5 p_T^{-1.183} \exp\left[-0.16\left(p_T^2 + 9.61\right)\right] \quad \text{for } 1.2 < |y| < 2.2 \tag{7}$$

For deriving the Expressions (6) and (7) we have used the relation $x \simeq \frac{2p_{z\mathrm{cm}}}{\sqrt{s}} = \frac{2m_T \sinh y_{\mathrm{cm}}}{\sqrt{s}}$ [14], where m_T, y_{cm} are the transverse mass of the produced particles and the rapidity distributions. $m_{J/\Psi} \simeq 3096.9 \pm 0.011$ MeV [14] and $B_{ll'}$, the branching ratio is for muons or electrons *i.e.* for lepton pairs $J/\Psi \to \mu^+\mu^-/e^+e^-$ is taken as $5.93 \pm 0.10 \times 10^{-2}$ [14] in calculating the above equations.

In a similar fashion, the total inclusive cross-sections for the production of *J*/Ψ-mesons in different rapidities (*i.e.*, $|y| < 0.75$ and $2.5 < |y| < 0$ respectively) in $p + p$ collisions at $\sqrt{s_{NN}}$ = 7 TeV at LHC would be,

$$\left.\frac{d^2\sigma}{\mathrm{d}p_T\mathrm{d}y}\right|_{p+p\to J/\Psi+X} = 78.5\,p_T^{-3.135}\exp\left[-0.013\left(p_T^2+9.61\right)\right] \quad \text{for } |y|<0.75 \tag{8}$$

and

$$\left.\frac{d^2\sigma}{\mathrm{d}p_T\mathrm{d}y}\right|_{p+p\to J/\Psi+X} = 37.5\,p_T^{-3.135}\exp\left[-0.016\left(p_T^2+9.61\right)\right] \quad \text{for } 2.5<|y|<0 \tag{9}$$

For the calculation of the rapidity distribution from the Equation (4) we can make use of a standard relation as given below:

$$\frac{\mathrm{d}N}{\mathrm{d}y} = \int \frac{1}{2\pi p_T}\frac{d^2N}{\mathrm{d}p_T\mathrm{d}y}\mathrm{d}p_T \tag{10}$$

For $p + p$ collisions, the calculated rapidity distribution equation at RHIC-energy $\sqrt{s_{NN}} = 200$ GeV is

$$\left.\frac{\mathrm{d}N}{\mathrm{d}y}\right|_{p+p\to J/\Psi+X} = 1.215\times10^{-6}\exp\left(-0.23\sinh y_{\mathrm{cm}}\right), \tag{11}$$

In a similar fashion, the SCM-based rapidity distribution equation at LHC-energy $\sqrt{s_{NN}} = 7$ TeV in $p + p$ collisions has been given hereunder

$$\left.\frac{\mathrm{d}N}{\mathrm{d}y}\right|_{p+p\to J/\Psi+X} = 8.025\exp\left(-0.043\sinh y_{\mathrm{cm}}\right). \tag{12}$$

4.2. Invariant Yields in *d* + *Au*, *Cu* + *Cu* and *Au* + *Au* Collisions at RHIC-Energy $\sqrt{s_{NN}} = 200$ GeV

From the expression (4), we arrive at the invariant yields for the J/Ψ production in $d + Au \to J/\Psi + X$ reactions for mid and forward-rapidities.

$$\left.\frac{1}{2\pi p_T}\frac{d^2N}{\mathrm{d}p_T\mathrm{d}y}\right|_{d+Au\to J/\Psi+X} = 7.3\times10^{-7}\,p_T^{-0.629}\exp\left[-0.13\left(p_T^2+9.61\right)\right] \quad \text{for } |y|<0.35 \tag{13}$$

and

$$\left.\frac{1}{2\pi p_T}\frac{d^2N}{\mathrm{d}p_T\mathrm{d}y}\right|_{d+Au\to J/\Psi+X} = 4.3\times10^{-7}\,p_T^{-0.629}\exp\left[-0.16\left(p_T^2+9.61\right)\right] \quad \text{for } 1.2<|y|<2.2 \tag{14}$$

For the case of *Cu* + *Cu* most central collisions (0% - 20%) at RHIC, the SCM-based calculated theoretical invariant yields for the rapidities $|y|<0.35$ and $1.2<|y|<2.2$ are given by the following equations respectively;

$$\left.\frac{1}{2\pi p_T}\frac{d^2N}{\mathrm{d}p_T\mathrm{d}y}\right|_{Cu+Cu\to J/\Psi+X} = 6.4\times10^{-5}\,p_T^{-0.829}\exp\left[-0.13\left(p_T^2+9.61\right)\right] \quad \text{for } |y|<0.35, \tag{15}$$

and

$$\left.\frac{1}{2\pi p_T}\frac{d^2N}{\mathrm{d}p_T\mathrm{d}y}\right|_{Cu+Cu\to J/\Psi+X} = 6.38\times10^{-5}\,p_T^{-0.829}\exp\left[-0.16\left(p_T^2+9.61\right)\right] \quad \text{for } 1.2<|y|<2.2. \tag{16}$$

Similarly, for *Au* + *Au* collisions at $\sqrt{s_{NN}} = 200$ GeV at RHIC, the equations of transverse momenta spectra for 0% - 20% centrality regions are given by the undernoted relations.

$$\left.\frac{1}{2\pi p_T}\frac{d^2N}{\mathrm{d}p_T\mathrm{d}y}\right|_{Au+Au\to J/\Psi+X} = 1.32\times10^{-3}\,p_T^{-1.023}\exp\left[-0.13\left(p_T^2+9.61\right)\right] \quad \text{for } |y|<0.35, \tag{17}$$

and

$$\left.\frac{1}{2\pi p_T}\frac{d^2N}{\mathrm{d}p_T\mathrm{d}y}\right|_{Au+Au\to J/\Psi+X} = 0.91\times10^{-3}\,p_T^{-1.023}\exp\left[-0.16\left(p_T^2+9.61\right)\right] \quad \text{for } 1.2<|y|<2.2. \tag{18}$$

For calculating the values of *NR*, in general, we have used the values of $\langle N_{\mathrm{part}}\rangle$ from Refs. [11] and [15].

4.3. The Nuclear Modification Factor R_{AB}

There is yet another very important observable called nuclear modification factor (NMF), denoted here by R_{AA} which for the production of J/Ψ is defined by [16]

$$R_{AA} = \frac{d^2\,N_{J/\Psi}^{AA}/\mathrm{d}p_T\mathrm{d}y}{\langle N_{\mathrm{coll}}(b)\rangle d^2\,N_{J/\Psi}^{pp}/\mathrm{d}p_T\mathrm{d}y} \tag{19}$$

The SCM-based results on NMFs for *Cu* + *Cu* and *Au* + *Au* collisions for forward rapidities are deduced on the basis of Equation (6), Equation (15), Equation (17) and Equation (19) and they are given by the undernoted relations

$$R_{AA}\big|_{Cu+Cu\to J/\Psi+X} = 0.42\,p_T^{0.35}, \tag{20}$$

and

$$R_{AA}\big|_{Au+Au\to J/\Psi+X} = 0.36\,p_T^{0.16}. \tag{21}$$

herein the value of $\langle N_{coll}(b)\rangle$ to be used is $\approx 170.5\pm11$ [17] for *Cu* + *Cu* collisions and for *Au* + *Au* collisions it is taken as $\approx 955.4\pm93.6$ [18].

4.4. Analysis of the Figures

In **Figures 1(a)** and **(b)**, we have drawn the total inclusive cross-sections for the production of *J*/Ψ-mesons in $p + p$ collisions in different rapidities at RHIC and LHC energies $\sqrt{s_{NN}}$ = 200 GeV and 7 TeV respectively. The solid lines in the figures are depicting the SCM model-based results with the help of the Equations (6)-(9) while the experimental measurements are taken from Ref. [19, 20] respectively.

In **Figure 2** we have plotted the rapidity distributions for *J*/Ψ-production in $p + p$ collisions at $\sqrt{s_{NN}}$ = 200 GeV. Data in the figure are taken from Ref. [21] and the line shows the SCM-based output.

Similarly, in **Figure 3**, we have drawn the rapidity distribution $\mathrm{d}n/\mathrm{d}y$ for *J*/Ψ production in $p + p$ collisions at $\sqrt{s_{NN}}$ = 7 TeV as function of y. The solid lines depict the SCM-based results [Equation (12)] and the points indicate the experimental measurements [22].

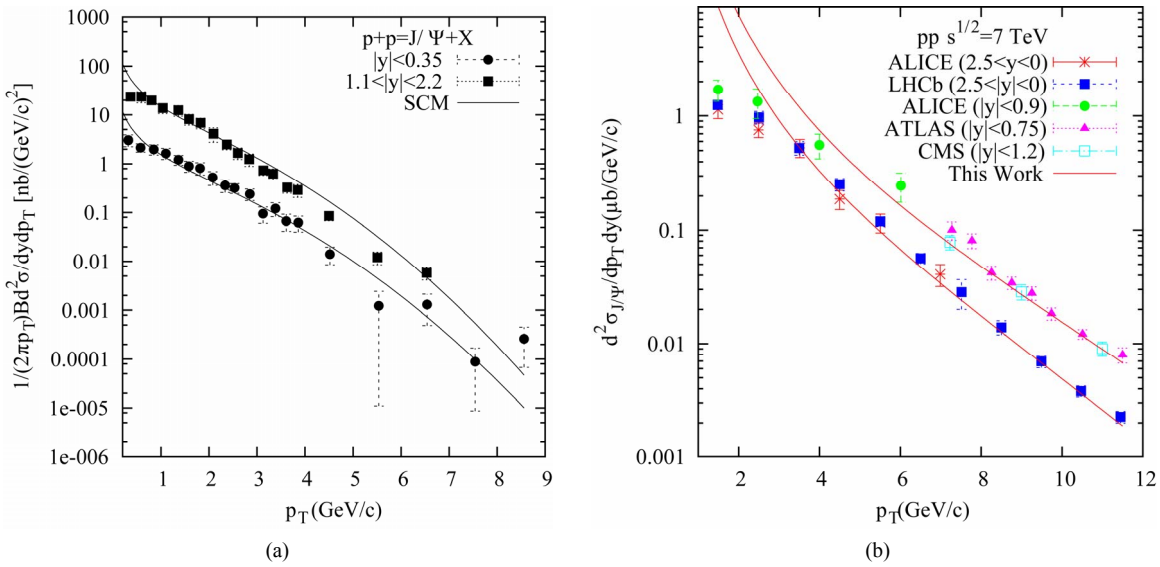

Figure 1. Plot of the invariant cross-section for *J*/Ψ production in proton-proton collisions at (a) $\sqrt{s_{NN}}$ = 200 GeV and (b) $\sqrt{s_{NN}}$ = 7 TeV as function of p_T. The data points are from [19] for (a) and from [20] for (b). The solid curves show the SCM-based results.

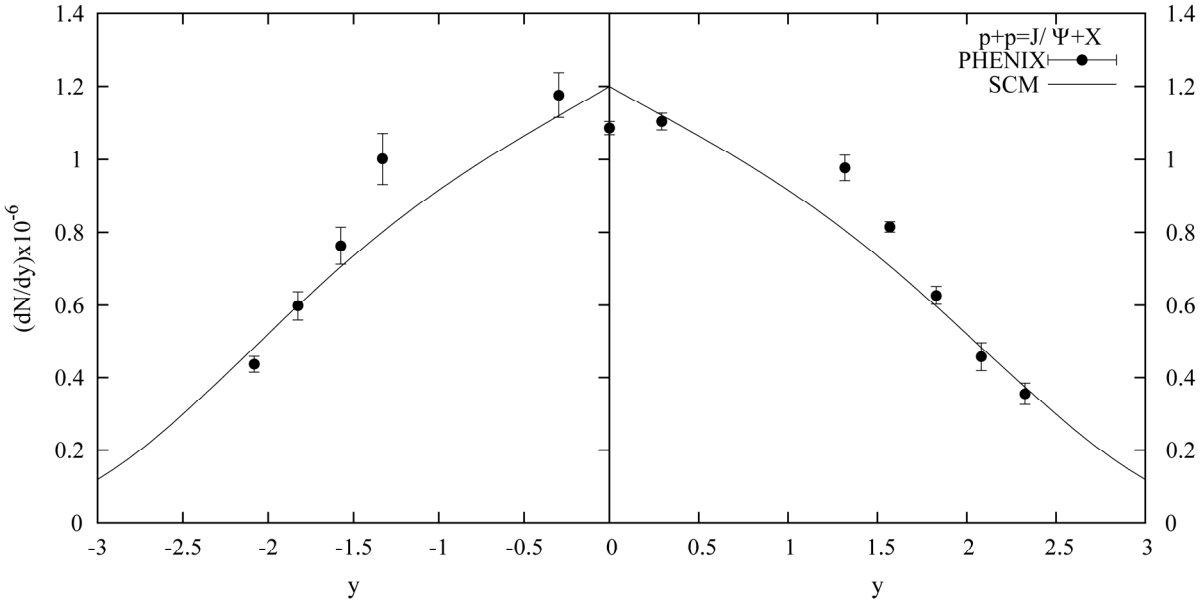

Figure 2. Plot of the rapidity distribution for *J*/Ψ production in proton-proton collisions at $\sqrt{s_{NN}}$ = 200 GeV as function of *y*. The data points are from [15,21]. The solid curves show the SCM-based results (Equation (11)).

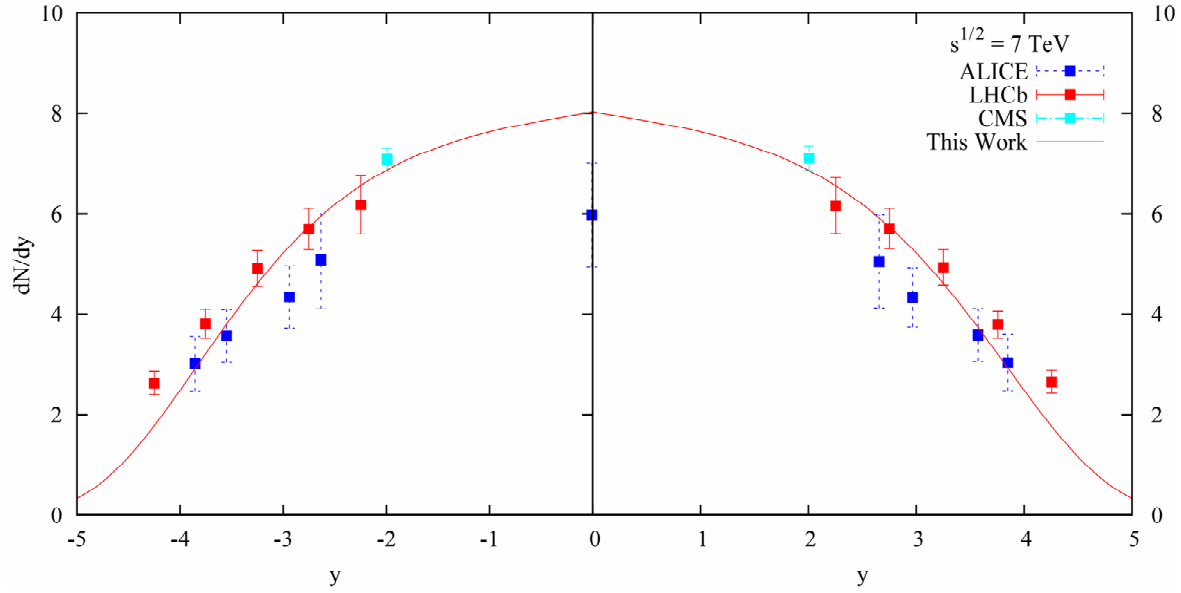

Figure 3. Plot of the rapidity distribution for *J/Ψ* production in *p* + *p* collisions at $\sqrt{s_{NN}}$ = 7 TeV as function of *y*. The data points are from [22]. The solid curves show the SCM-based results (Equations (15) and (16)).

In **Figure 4**, we have drawn the solid lines depicting the SCM-based results for invariant yields for *J/Ψ* production in *d* + *Au* collisions at $\sqrt{s_{NN}}$ = 200 GeV with the help of two Equations (13) and (14) against the experimental measurements [15].

The experimental results for the invariant yields of *J/Ψ* production as a function of transverse momenta for *Cu* + *Cu* collisions at $\sqrt{s_{NN}}$ = 200 GeV are taken from Ref. [16] at centrality 0% - 20% and are plotted in **Figure 5**. The solid lines in the figure show the SCM-induced results.

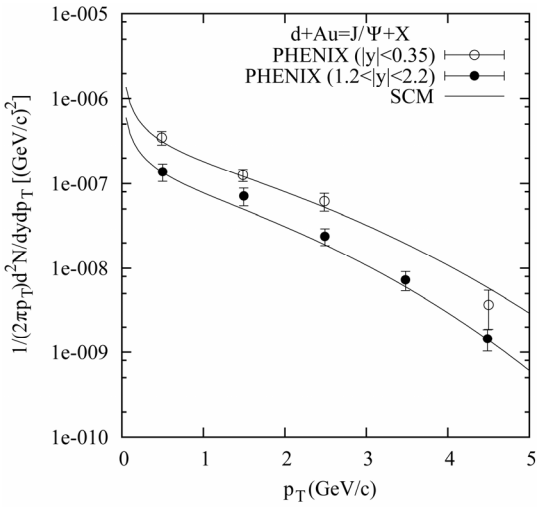

Figure 4. Plot of the invariant yields for *J/Ψ* production in *d* + *Au* collisions at $\sqrt{s_{NN}}$ = 200 GeV as function of p_T. The data points are from [15]. The solid curves show the SCM-based results.

In the **Figure 6**, the solid lines are the plots of SCM-based invariant yields vs. p_T as described by Equations (17) and (18) at forward and mid-rapidities for *Au* + *Au* collisions at $\sqrt{s_{NN}}$ = 200 GeV, while the dotted curve in the Fig. shows results of coalescence model [12]. The experimental data points in the **Figure 6** for the invariant yields of *J/Ψ* production as a function of transverse momenta at centrality values 0% - 20% and at the rapidities $|y| < 0.35$ and $1.2 < |y| < 2.2$ respectively are taken from the PHENIX Collaboration [15].

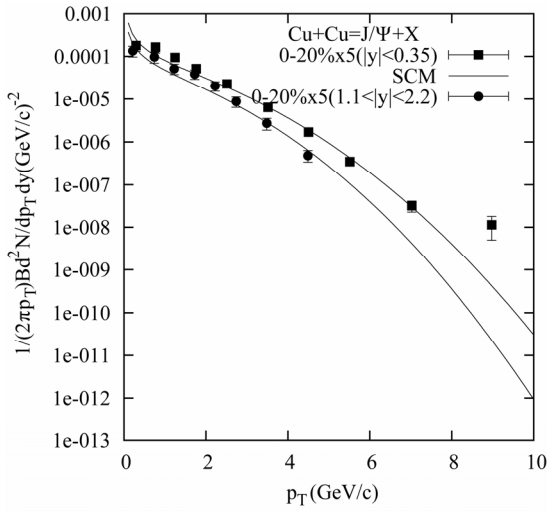

Figure 5. Transverse momenta spectra at $|y| < 0.35$ and $1.2 < |y| < 2.2$ for *J/Ψ* production in *Cu* + *Cu* central collisions at $\sqrt{s_{NN}}$ = 200 GeV. The data are taken from [16]. The solid curves depict the SCM-based results.

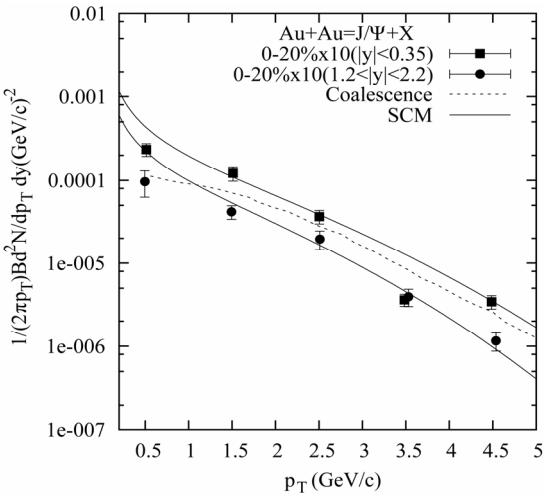

Figure 6. Plot of the invariant yields for *J/Ψ* production in *Au* + *Au* collisions at $\sqrt{s_{NN}}$ = 200 GeV as function of p_T. The data points are from [21]. The solid curve shows the SCM-based results while the dotted curve depicts the Coalescence Model [12].

In **Figure 7(a)**, we plot R_{AA} vs. p_T for 0% - 20% central region in *Cu* + *Cu* and *Au* + *Au* collisions at $\sqrt{s_{NN}}$ = 200 GeV. The solid lines in the figure show the SCM-based results (Equations (20) and (21)) against the experimentally measured results [15,16]. The dotted lines in the figure. represent the double Color Filtering approach [13].

And in **Figure 7(b)**, we plot R_{AA} vs. N_{part} for 0% - 20% central region in *Au* + *Au* collisions at $\sqrt{s_{NN}}$ = 200 GeV and for *Pb* + *Pb* collisions at $\sqrt{s_{NN}}$ = 2.76 TeV. The solid lines in the figure show the SCM-based calculations for different <N_{part}>'s. The Values of <N_{part}>'s are taken from Ref. [17]. The the experimentally measured results from Refs. [11,23] respectively. The dashed lines in the figure. represent the Gluon Saturation approach [11].

5. Summary and Outlook

Let us first concentrate on what we have achieved here: 1) The features related to p_T—spectra for *J/Ψ* production in some particle-particle and nuclear collisions at various high energies have been reproduced quite successfully; 2) The characteristics of rapidity spectra in *p* + *p* collisions at TeV energies have been brought out somewhat modestly satisfactorily; 3) The features of nuclear modification factors in *Cu* + *Cu*, *Au* + *Au* and *Pb* + *Pb* reactions at RHIC and LHC energies have also been brought out with the help of the applied model. Besides, some of our model-based results have also been compared with the performances on the same observables by some competing models of "standard" variety. And these comparisons with data and the results obtained by some other models reveal that SCM-based results describe the features of the data, at least, not inferior to the performance by the other approaches grounded on the "Standard" model ilk. In the past such were the recurrent observations made by us valid for many other obsevables measured in the various high statistics high energy particle and nuclear experiments.

Thus, summing up our past experiences and consider-

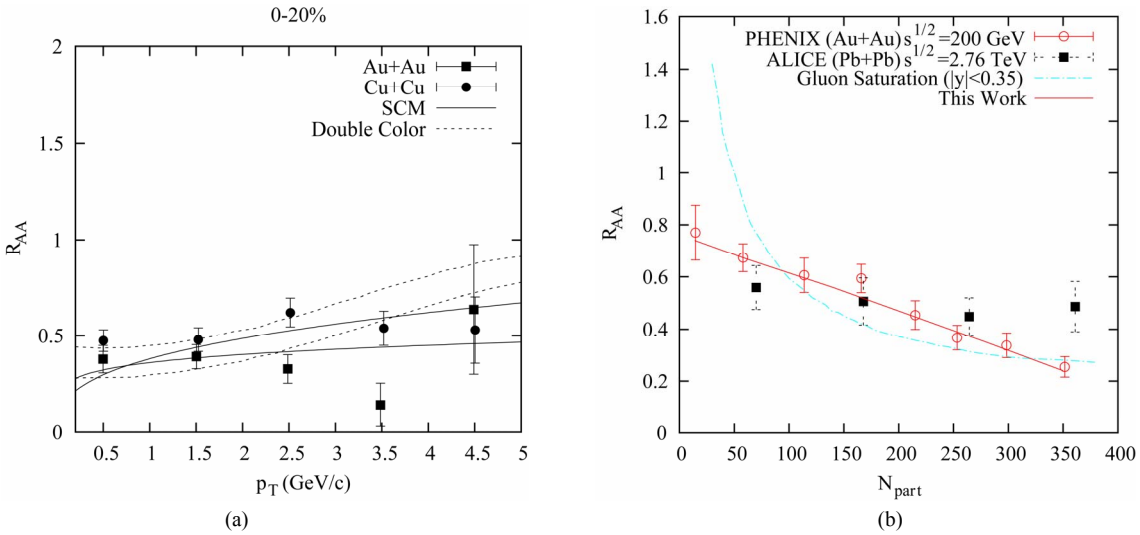

Figure 7. (a) Plot of the R_{AA} for *J/Ψ* production in *Cu* + *Cu* and *Au* + *Au* collisions at $\sqrt{s_{NN}}$ = 200 GeV as function of p_T. The data points are from [15,16]. The solid and dotted curves show respectively the SCM and the Double Color Filter-oriented [13] results. (b) Plot of the R_{AA} vs. N_{part} for *J/Ψ* production in *Au* + *Au* collisions at $\sqrt{s_{NN}}$ = 200 GeV and *Pb* + *Pb* collisions at $\sqrt{s_{NN}}$ = 2.76 TeV. The red circles depict *Au* + *Au* collisions [11] while the black squares represent *Pb* + *Pb* collisions [23]. The solid curves show the SCM-based results while the dotted curve depicts the Gluon Saturation Approach [11].

ing the weightage of the results reported here, we are forced to comment finally that this work essentially represents a case of paradigm shift in the domain of particle theory, as we have eschewed the conventional views of $c\bar{c}$ approach to J/Ψ production in the "standard" framework. And this is just the reflection of our radical views about the particle structure and the nature of particle collisions. Obviously we obtain the fair agreement with data on some observables without inductions of 1) any QGP concept; 2) any prognosis of suppression or enhancement of J/Ψ-production. The production of J/Ψ-particles resembles all other hadrons.

6. Acknowledgements

The authors would like to express their thankful gratitude to the learned Referee for his/her valuable remarks and constructive suggestions in improving the earlier draft of the manuscript.

REFERENCES

[1] T. Matsui and H. Satz, "J/Ψ Suppression by Quark-Gluon Plasma Formation," *Physics Letters B*, Vol. 178, No. 4, 1986, pp. 416-422. doi:10.1016/0370-2693(86)91404-8

[2] R. L. Thews and M. L. Mangano, "Momentum Spectra of Charmonium Produced in a Quarkgluon Plasma," *Physical Review C*, Vol. 73, No. 1, 2006, Article ID: 014904. doi:10.1103/PhysRevC.73.014904

[3] P. Guptaroy, B. De, G. Sanyal and S. Bhattacharyya, "J/Ψ Production in High Energy Particle and Nuclear Collisions: Suppressed, Enhanced or Just Normal?" *International Journal of Modern Physics A*, Vol. 20, No. 20-21, 2005, pp. 5037-5058. doi:10.1142/S0217751X05020768

[4] P. Guptaroy, T. K. Garain and S. Bhattacharyya, "J/Ψ Production in Some RHIC Interactions at $\sqrt{s_{NN}}$ = 200 GeV and the Look into the System Size Effect," *Hadronic Journal*, Vol. 31, No. 5, 2008, p. 451.

[5] P. Guptaroy, T. K. Garain, Goutam Sau, S. K. Biswas and S. Bhattacharyya, "Analysing J/Ψ Production in Various RHIC Interactions with a Version of Sequential Chain Model (SCM)," *Hadronic Journal*, Vol. 32, No. 1, 2009, p. 95.

[6] S. Bhattacharyya, "Collisions in Space Experiments at High-Energies, Laboratory Experiments and Suggested Signatures of Quark Gluon-Plasma: An Alternative Approach to the Analysis of Actual Observations," *IL Nuovo Cimento C*, Vol. 11, No. 1, 1988, pp. 51-65. doi:10.1007/BF02507895

[7] P. Guptaroy, G. Sau, S. K. Biswas and S. Bhattacharyya, "Understanding the Characteristics of Multiple Production of Light Hadrons in Cu + Cu Interactions at Various RHIC Energies—A Model-Based Analysis," *IL Nuovo Cimento B*, Vol. 125, No. 9, 2010, p. 1071.

[8] P. Guptaroy, G. Sau, S. K. Biswas and S. Bhattacharyya, "On Production of Direct Photons and Neutral Pions in RHIC Experiments at $\sqrt{s_{NN}}$ = 200 GeV," *Modern Physics Letters A*, Vol. 23, No. 14, 2008, pp. 1031-1046. doi:10.1142/S021773230802567X

[9] S. Bhattacharyya, "On Some Remarkable Differences between the pp Collider Results at CERN and pp Reaction at ISR Energies," *Journal of Physics G*, Vol. 14, No. 1, 1988, pp. 9-17. doi:10.1088/0305-4616/14/1/005

[10] C. Y. Wong, "Introduction to High-Energy Heavy Ion Collisions," World Scientific, Singapore, 1994. doi:10.1142/9789814277549

[11] A. Adare, *et al.*, "J/Ψ Suppression at Forward Rapidity in Au + Au Collisions at $\sqrt{s_{NN}}$ =200 GeV," *Physical Review C*, Vol. 84, No. 5, 2011, Article ID: 054912.

[12] D. E. Kahana and S. H. Kahana, "J/Ψ Production by Charm Quark Coalescence," *Journal of Physics G*, Vol. 37, No. 11, 2010, Article ID: 115011. doi:10.1088/0954-3899/37/11/115011

[13] B. Z. Kopeliovich, "Puzzles of J/Ψ Production off Nuclei," *Nuclear Physics A*, Vol. 854, No. 1, 2011, pp. 187-197.

[14] K. Nakamura, *et al.*, "Review of Particle Physics," *Journal of Physics G*, Vol. 37, No. 7A, 2010, Article ID: 075021. doi:10.1088/0954-3899/37/7A/075021

[15] A. Adare, *et al.*, "Cold Nuclear Matter Effects on J/Ψ Production as Constrained by Deuteron-Gold Measurements at $\sqrt{s_{NN}}$ =200 GeV," *Physical Review C*, Vol. 77, No. 2, 2008, Article ID: 024912. doi:10.1103/PhysRevC.77.024912

[16] A. Adare, *et al.*, "J/Ψ Production in $\sqrt{s_{NN}}$ =200 GeV Cu + Cu Collisions," *Physical Review Letters*, Vol. 101, No. 12, 2008, Article ID: 122301. doi:10.1103/PhysRevLett.101.122301

[17] B. Alver, *et al.*, "System Size and Centrality Dependence of Charged Hadron Transverse Momentum Spectra in Au + Au and Cu + Cu Collisions at $\sqrt{s_{NN}}$ = 62.4 and 200 GeV," *Physical Review Letters*, Vol. 96, No. 21, 2006, Article ID: 212301. doi:10.1103/PhysRevLett.96.212301

[18] S. S. Adler, *et al.*, "Identified Charged Particle Spectra and Yields in Au + Au Collisions at $\sqrt{s_{NN}}$ = 200 GeV," *Physical Review C*, Vol. 69, No. 3, 2004, Article ID: 034909. doi:10.1103/PhysRevC.69.034909

[19] A. Adare, *et al.*, "J/Ψ Production versus Transverse Momentum and Rapidity in p + p Collisions at $\sqrt{s}$ =200 GeV," *Physical Review Letters*, Vol. 98, No. 23, 2007, Article ID: 232002. doi:10.1103/PhysRevLett.98.232002

[20] G. M. García, "Quarkonium Production Measurements with the ALICE Detector at the LHC," *Journal of Physics G*, Vol. 37, No. 9, 2010, Article ID: 094051.

[21] A. Adare, *et al.*, "Cold Nuclear Matter Effects on J/Ψ Yields as a Function of Rapidity and Nuclear Geometry in Deuteron-Gold Collisions at $\sqrt{s_{NN}}$ = 200 GeV," 2010. arXiv:1010.1246v1 [nucl-ex]

[22] R. Arnaldi, "Measurement of J/Ψ Production in pp Collisions at $\sqrt{s}$ = 2.76 and 7 TeV with ALICE," *Journal of Physics G*, Vol. 38, No. 12, 2011, Article ID: 124106. doi:10.1088/0954-3899/38/12/124106

[23] P. Pillot, "J/Ψ Production at Forward Rapidity in Pb-Pb Collisions at $\sqrt{s_{NN}}$ = 2.76 TeV, Measured with the ALICE Detector," *Journal of Physics G*, Vol. 38, No. 12, 2011, Article ID: 124111. doi:10.1088/0954-3899/38/12/124111

